Optical Materials 51 (2016) 31–34

Contents lists available at ScienceDirect

Optical Materials

journal homepage: www.elsevier.com/locate/optmat

Optical waveguides in Yb:SBN crystals fabricated by swift C^{3+} ion irradiation

Guiyuan Liu [a,d], Ningning Dong [b], Jun Wang [b], Shavkat Akhmadaliev [c], Shengqiang Zhou [c], Feng Chen [a,*]

[a] School of Physics, State Key Laboratory of Crystal Materials and Key Laboratory of Particle Physics and Particle Irradiation (MOE), Shandong University, Jinan 250100, China
[b] Key Laboratory of Materials for High-Power Laser, Shanghai Institute of Optics and Fine Mechanics, Chinese Academy of Sciences, Shanghai 201800, China
[c] Helmholtz-Zentrum Dresden-Rossendorf, Institute of Ion Beam Physics and Materials Research, Dresden 01314, Germany
[d] School of Science, Shandong Jianzhu University, Jinan 250101, China

ARTICLE INFO

Article history:
Received 27 August 2015
Received in revised form 11 November 2015
Accepted 13 November 2015
Available online 21 November 2015

Keywords:
Optical waveguides
Yb:SBN crystal
Ion implantation
Confocal photoluminescence

ABSTRACT

We report on the fabrication of optical planar waveguides supporting both the TE and TM confinements in Yb:SBN crystal by swift C^{3+} ions irradiation. A combination of the micro-photoluminescence and micro-Raman investigations have evidenced the presence of lattice distortion, damage and disordering of the SBN network along the ion irradiation path, with these effects being at the basis of the refractive index modification. The enhanced micro-photoluminescence and micro-Raman intensity in the waveguide volumes show the potential application of the obtained waveguides as active laser gain media.

1. Introduction

Ytterbium doped strontium barium niobate crystal [$Sr_xBa_{(1-x)}Nb_2O_6$ with $0.4 < x < 0.8$, hereafter Yb:SBN] has becoming an excellent optical material in photonics owing to the combination of outstanding fluorescence of Yb^{3+} ions (such as long fluorescence lifetime, absence of excited state absorptions from the metastable state, broad emission bands, high emission and absorption cross sections) and the excellent photorefractive, electro-optic, nonlinear optic, and dielectric properties of SBN [1–4]. In integrated optics, optical waveguides offer unique platforms for light confinement and steering in chip-scale devices [5]. Owing to the small geometries of the order of micrometers, relatively high optical intensities could be reached in waveguides with respect to bulks. This feature enables enhanced performance of bulk materials in compact volumes [6,7]. For example, waveguide lasers possess reduced lasing thresholds and enhanced efficiencies [8–10]; and the frequency conversion in guided-wave manner may have improved performance [11–13]. The rare-earth (RE) doped crystals are ideal gain media for active applications, e.g., lasing and amplifications of optical signals. Optical waveguides have been produced in RE doped crystals by a few well-developed techniques, receiving a number of intriguing applications [14]. Different from the chemical methods (such as metal ion thermal indiffusion and ion exchange), the "physical" techniques like ultrafast laser writing [15–18] and ion irradiation [19–22] are most suitable for direct engineering the refractive index changes of the optical crystals. The ion irradiation is more advantageous than ultrafast laser writing on the large-area device production. The energetic ion beams create lattice modifications of the crystals through the energy depositions. In the typical light ion implantation, the nuclear collisions are dominant and the required refractive index changes for waveguide construction are mainly due to the nuclear damage [19]. In typical swift heavy ion irradiation regimes, the ion excitation induced electronic damage plays the main role, and in low-fluence case, the nuclear damage is negligible [20]. In the regimes between these two domains, the refractive index changes may be the synergy effect of both electronic and nuclear contributions [23–25]. In addition, the boundary for regimes of different ion irradiations is strongly depended on the material properties and the ion fluences. Owing to these advantages, researchers have successfully produced optical waveguides in more than 100 optical materials by applying ion irradiation with diverse parameters [19–22]. Particularly, the waveguides in SBN and KNSBN crystals have been manufactured by irradiation of He, Cu ions, etc. [26–28]. In this work, we focus on the Yb^{3+} ion doped SBN crystal, and investigate the fabrication and micro-fluorescence and micro-Raman properties of the waveguides. With the data obtained from the confocal spectra, the micro-structural modification in the crystal induced by the ion irradiation is investigated.

---

* Corresponding author.
E-mail address: drfchen@sdu.edu.cn (F. Chen).

http://dx.doi.org/10.1016/j.optmat.2015.11.019
0925-3467/

2. Experimental

The Yb:SBN crystal (doped by 0.75 mol% Yb^{3+} ions, $x = 0.61$) used in this work was a $5 \times 5 \times 10\ mm^3$ prism and optically polished. An optical planar waveguide has been produced by C^{3+} ion irradiation on one $5 \times 10\ mm^2$ surface at energy of 15 MeV and fluence of $4 \times 10^{14}\ cm^{-2}$ through the 3 MV tandem accelerator at Helmholtz-Zentrum Dresden-Rossendorf, Germany. The ion current was kept to be as low as ~10 nA to avoid thermal effects.

The transmission properties of the waveguide were performed by a typical end-face coupling arrangement with a linearly polarized He–Ne laser at 632.8 nm as the probe light source [21]. By adjusting the polarization of the probe light beam, both TE and TM polarized model profiles were obtained. In addition, the propagation loss measurement could be performed based on this arrangement by directly measuring the input and output light power through the waveguides and then calculated by considering a few parameters, i.e., the launching coupling efficiency, Fresnel reflections at the input air/waveguide interface (~11% per interface), absorption of bulk materials at the probe light wavelength. With this arrangement, the propagation loss could be determined [21]. In order to study the nature and spatial location of the modified volumes, an Olympus BX-41 fiber-coupled confocal microscope was used to investigate the micro-photoluminescence (μ-PL) and μ-Raman properties of the waveguide. The sample was mounted on an XY motorized stage with a spatial resolution of 100 nm. The μ-PL measurements were performed by using a mode locked Ti:Sapphire laser providing 100 fs pulses at a repetition rate of 80 MHz. The 900 nm fs laser was focused onto the cross section by using a 100 × (N.A. = 0.8) microscope objective. The back-scattered PL signals were collected with the same objective and, after passing through a series of filters and a confocal aperture, were collected by a fiber-coupled spectrometer. The μ-Raman measurements were performed with the same setup but with another 100 × (N.A. = 0.9) microscope objective and the excitation laser was a 488 nm argon laser. In this case, a set of notch filters were placed between the focusing objective and the confocal aperture.

3. Results and discussions

The refractive index (n) of C^{3+} irradiated waveguide has a typical "well" + "barrier" type distribution. A positive change $\Delta n_w \approx +0.008$ and a negative variation $\Delta n_b \approx -0.025$ have been determined in the C^{3+} irradiated sample surface (well) and the boundary of the waveguide and substrate (barrier), respectively. For further understanding of the implantation-induced modifications in the crystal, we simulated the energy deposition process of the swift C^{3+} ion irradiation into the Yb:SBN crystal with the software Stopping and Range of Ions in Matter (SRIM) 2010 code. The corresponding electronic and nuclear stopping power profiles (S_e and S_n) are depicted in Fig. 1. It seems reasonable that the optical well and barrier are induced by the electronic collisions and nuclear collisions, respectively. In addition, the maximum of S_e is about 2.1 keV/nm at depth of ~6 μm below the sample surface; however, S_n increases to one peak of 0.17 keV/nm at about 8.5 μm at the end of C^{3+} ion projected range.

Fig. 2(a) shows an transmission photograph of the end-face of the 15 MeV C^{3+} ion irradiated Yb:SBN. As we can see, the waveguide vertical depth is about 7 μm, which is consistent with the mean projected range of the C^{3+} ion based on the SRIM calculation. The optical propagation properties of the obtained planar waveguide at wavelength of 632.8 nm were performed with a He–Ne laser. Fig. 2(b) and (c) shows the near field distributions of the guided TE and TM modes, respectively. The waveguide loss is estimated to be of ~2 dB/cm, which is comparable to those obtained in He or H ion implanted SBN waveguides [6,21].

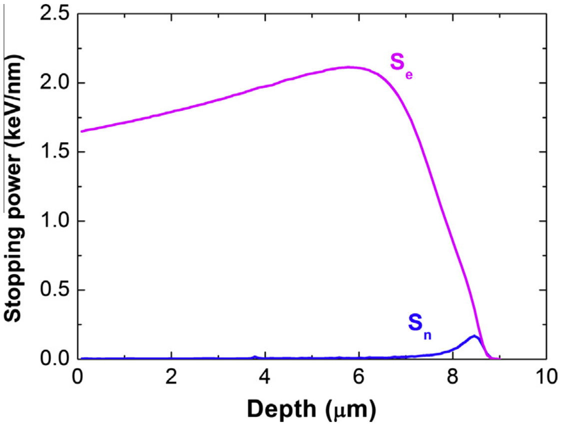

Fig. 1. The electronic and nuclear stopping power curves (S_e and S_n) of 15 MeV C^{3+} ion in Yb:SBN crystal as functions of penetration depth from the irradiated sample surface.

In order to obtain a better understanding of the microstructural modifications induced in the C^{3+} ion irradiated Yb:SBN network, we have performed the confocal microscopy to analyze the fluorescence properties. The emitted luminescence at room temperature obtained from the bulk Yb:SBN crystal excited by 900 nm femtosecond laser is same as the result of Rodríguez et al. [29]. The emission spectra of Yb^{3+} ions from the bulk and waveguide are quite similar in respect to the intensity of emissions. To investigate the detailed modification of the Yb^{3+} emissions, we focus on the 975 nm emission line, which is fitted in order to extract its intensity, spectral position and width. Fig. 3(a)–(c) shows the obtained 2D μ-PL images based on the spatial distribution of the intensity, spectral shift and broadening of this emission line, respectively. In order to give a clear presentation, we also provide the 1D profiles as a function of in-depth (see Fig. 3(d)–(f)). As we can see, within the first 1 μm, the luminescence intensity, energy shift and line broadening show nearly no relevant changes with respect to the bulk area which means the C^{3+} ion irradiation has negligible influence on the Yb:SBN crystal network in these area. In addition, the luminescence has strong enhancements in the range of 1–7 μm under the sample surface, which indicates the spectroscopic properties of the Yb^{3+} ions are well preserved in the planar waveguide and this is an advantageous feature for laser applications. At the same time, apparent red shifts and spectral broadening can be observed at the waveguide volumes. As it has been discussed in our prior works [30–32], the Yb:SBN network has been strongly distorted in the waveguide volume as the main result of electronic collisions. Whereas, weaker luminescence quenching, smaller blue shifts and slight line broadening are observed in the barrier areas (7–14 μm). These indicate that some damage/disordering and slight distortion have been produced in the barrier as a consequence of nuclear collisions.

In order to get a deeper knowledge of the structural changes induced during the C^{3+} ion irradiation, μ-Raman spectra were analyzed. Fig. 4(a) depicts a typical confocal μ-Raman spectrum obtained from the bulk of the Yb:SBN crystal [33]. In this spectrum, three broad features at about $170\ cm^{-1}$, $621\ cm^{-1}$ and $830\ cm^{-1}$ are observed. The first two strong bands can be attributed to δ(O–Nb–O) bending and ν(Nb–O) symmetric stretching vibrational modes, respectively. The weak $830\ cm^{-1}$ band is assigned to δ(O–Nb–O) bending vibrations [33]. We have focused our attention to the Raman mode at $621\ cm^{-1}$. Fig. 4(b)–(d) is the corresponding